Weak forces and conductance in the formation of a contact between two molecules

Martina Corso[1,2,3], Martin Ondráček[4], Christian Lotze[1], Prokop Hapala[4], Katharina J. Franke[1], Pavel Jelínek[4], and J. Ignacio Pascual[1,3,5]
[1] *Institut für Experimentalphysik, Freie Universität Berlin, 14195 Berlin, Germany.*
[2] *Centro de Fisica de Materiales CSIC/UPV-EHU, 20018 Donostia-San Sebastian, Spain.*
[3] *Ikerbasque, Basque Foundation for Science, 48011 Bilbao, Spain.*
[4] *Institute of Physics, Academy of Sciences of the Czech Republic, 162 00 Prague, Czech Republic.*
[5] *CIC nanoGUNE, 20018 Donostia-San Sebastian, Spain.*
(Dated: July 8, 2015)

The forces between two single molecules brought into contact, and their connection with charge transport through the molecular junction, are here studied using non contact AFM, STM, and DFT simulations. A carbon monoxide molecule approached to an acetylene molecule (C_2H_2) feels initially weak attractive electrostatic forces, partly arising from charge reorganization in the presence of molecular dipoles. We find that the molecular contact is chemically passive, and protects the electron tunneling barrier from collapsing, even in the limit of repulsive forces. However, we find subtle conductance and force variations at different contacting sites along the C_2H_2 molecule attributed to a weak overlap of their respective frontier orbitals.

PACS numbers: 68.37.Ps,34.20.Gj,73.63.Rt,74.55.+v

The formation of an atomic-sized contact between two solids is an intriguing problem in physics [1]. Basic properties of nanoscale solids and composite materials such as adhesion, friction, or electrical conductance depend on the nature of their contacts at the atomic level. At proximity length scales comparable to the atomic dimensions and the electronic Fermi wavelength, the onset of electrical and a mechanical contact can be independently defined and may occur at different atomic separations [2]. For example, electronic transport through atomic contacts in metals is ballistic before the mechanical contact (i.e. bond equilibrium position) because the strong hybridization of localized atomic orbitals precedes the point of mechanical stability [3]. Atomic-scale contacts may also endow the system with new properties. In covalent contacts between semiconductors or molecular radicals the hybridization of frontier orbitals may be accompanied by a strong re-distribution of charges, creating electrostatic barriers [4], or reducing the conductance of the contact [5, 6].

In contrast, the contact between (close-shell) molecules is weak and stabilized by van der Waals interactions. It thus has a larger bond equilibrium distance and the electrical conduction decreases due to smaller wave-function overlap [7]. The weak intermolecular forces are, however, highly sensitive to small changes of their surrounding electrostatic landscape and to structural rearrangements [7]. This is a key concept behind the electronic functionality of soft organic materials because charge hopping and electronic delocalization are determined by the overlap of the molecular orbitals [8].

In this work, we study the correlation of electrical transport and short-range forces during the formation of a weak contact between two molecules using simultaneously force and current measurements in a Scanning Tunneling Microscope. To create a robust molecular junction we use a carbon monoxide (CO) functionalized tips. These have shown to be stable at very short distances. Numerous studies resolved the chemical structure of adsorbed molecules with atomic and bond resolution [9–15] at the onset of Pauli repulsion forces. As counter electrode we used an acetylene molecule (C_2H_2) on a copper substrate. We find that weak attractive forces are enhanced by the formation of dipoles induced by the charge reorganization due to the proximity of the molecules. The interaction landscape is further correlated with the tunneling transmission of the junction. The two molecules behave as chemically passive spacers, with low transmission tunneling channels even when compressive forces are applied. However, contacting the acetylene at the C=C bond leads to relatively larger electrical transmission, confirming that electrical properties of organic systems are very sensitive to details on their structure.

We used a combined STM/nc-AFM based on a qPlus sensor design [16] operated in frequency modulation mode [17], at 5 K and in ultra-high vacuum [18]. We measured frequency shift Δf(x,z) plots, and determined the corresponding vertical force F_z(x,z) in the pN range using the Sader and Jarvis method [19]. To provide quantitative values of forces and energies between the molecules, we removed the Δf(x,z) background due to long-range forces between the metal tip and sample [20] (see supplementary material SM [21]). For simultaneous conductance measurements G(x,z), a small bias of 80 mV was applied [21].

Acetylene molecules were deposited on a clean Cu(111) surface at 130 K, together with a small amount of carbon monoxide (CO) molecules for functionalizing the tip-apex. On the Cu(111) surface, acetylene undergoes a strong hybridization which converts the central *sp* bond into a double bond and bends the hydrogen atoms up-

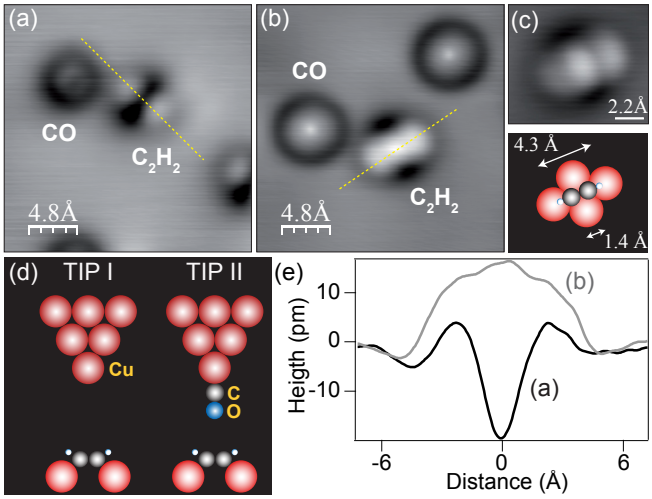

FIG. 1: (a, b) Constant current STM images taken on CO and C_2H_2 molecules in different sample positions at V=100 mV and I=0.15 nA. These images (a and b) were measured respectively with the tip terminations schematically drawn in (d): a sharp Cu tip (I) and a CO tip (II). The appearance of a C_2H_2 with a CO tip and its adsorption geometry from [22] are shown in (c). (e) Topography profiles taken along the yellow lines measured on the C_2H_2 in (a) and (b).

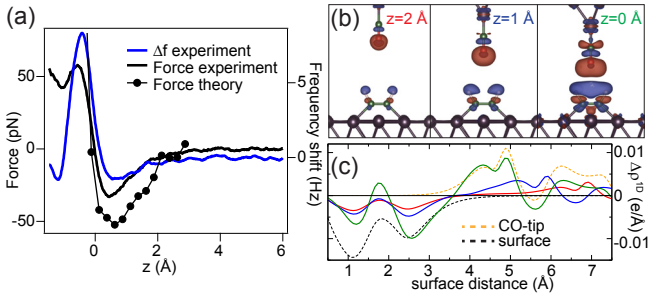

FIG. 2: (a) Frequency shift (Δf) and the corresponding vertical force [19] measured with a CO functionalized tip at V=0 mV as a function of the tip-sample distance (z) over the C=C bond of a C_2H_2 molecule (further details in [21]). Δf is corrected for the macroscopic influence of the tip as explained in [21]. The calculated force is included as dots for comparison. (b) Development of the induced electron density $\Delta\rho = \rho_{tot} - \rho_{surf} - \rho_{tip}$ and (c) its projection into z, $\Delta\rho^{1D} = \int\int \Delta\rho \; dxdy$ at three CO-acetylene distances. In (b) we plot $\Delta\rho$ isosurfaces at 0.0005 e/Å, where blue and red mean depletion and accumulation of electrons, respectively. Dashed black and yellow lines in (c) show induced electron density of non-interacting free standing acetylene-surface and CO-tip, when an electric field 0.1 eV/Å is applied.

wards (see Fig. 1d) [22]. We transferred a CO molecule to the apex of the STM tip as described in ref. [23]. In most cases, the CO molecule adopts a standing up configuration on the tip apex, exposing the oxygen atom outwards (Fig. 1d) [24].

The shape of acetylene in the STM images varies depending on the termination of the tip apex. Figure 1 compares constant current STM images obtained with a sharp copper tip (a) and with a CO-functionalized tip (b, c). In the first case (Fig. 1(a)) acetylene is imaged with a characteristic dumbbell shape [25, 26]. Using a CO functionalized tip the contrast of acetylene is reversed, and appears with a three lobed structure peaked by a central maximum, clearly visible in the line profile in Fig. 1(e). This is due to the symmetry enhanced tunneling contribution from CO p orbitals into π^* states of acetylene [27].

Electrostatic origin of short range forces: We first address the identification of the interaction forces between CO and acetylene molecules in close proximity. Figure 2 shows the frequency shift (Δf), and the integrated force as a function of their separation z [21]. Both molecules attract each other in a short distance range of ~ 2 Å and form a stable bond at z=0 Å. We defined this point (z_0) as the distance where short-range forces are relaxed ($F_z(z_0)$), i.e. the energy minimum or equilibrium bond distance. The maximum attractive force before that point reaches -33±5 pN. The bond created between the two species is clearly non-covalent, with binding energy of -70 ± 5 meV [21].

Repulsive (Pauli) forces build up in the junction when approaching the tip to closer positions. In this region a characteristic maxima in Δf can be observed, which gives rise to a small relaxation of forces at the junction [21]. As we shall show below, such relaxation can be attributed to the bending of the CO molecule at the tip.

To unveil the origin of the attractive molecular forces, we performed DFT-based simulations of the interaction between the two molecules adsorbed in their respective environment (details are given in the supplementary information [21]). The force simulations reproduce well the results of the AFM measurement (Fig. 2a), obtaining a maximal attractive force of 52 pN over the center of the C_2H_2 molecule. The force minimum is reach at a distance of 75 pm (50 pm in the experiment) before a relaxed bond is formed (F_z=0 point); thus it is a short range force. This force has two main components. A fraction of it is due to *molecular* London dispersion forces, amounting to 27.5 pN. The rest is due to electrostatic forces related to static dipoles and to the charge redistribution induced by the proximity of the molecules.

The origin of this last attractive force component can be tracked down by analyzing the induced charge density ($\Delta\rho$) due to the interaction between CO and C_2H_2 molecules. Figure 2b shows $\Delta\rho$ isosurfaces at three different CO-C_2H_2 separations, from the onset of attractive forces (z=2 Å) to the point of minimum energy, z_0. We observe in all the cases no trace of electron accumulation in the CO-C_2H_2 gap, supporting the absence of covalent character of the bond between the two molecules. However, there is a growing charge redistribution as the

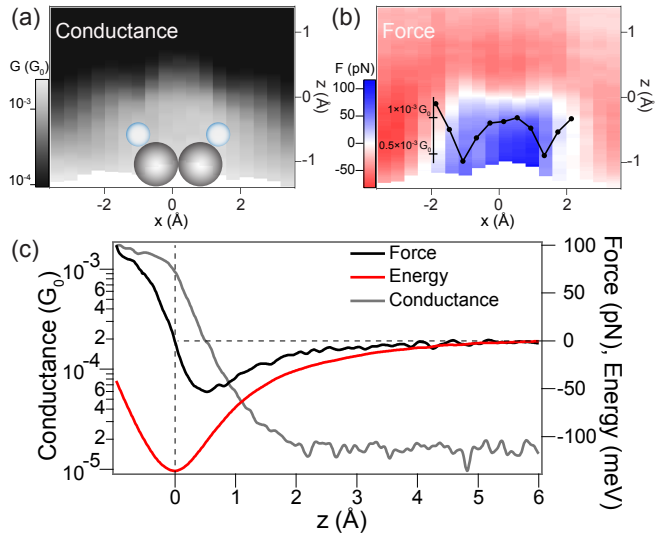

FIG. 3: (a-b) Conductance and force maps recorded simultaneously along a C_2H_2 molecular axis while applying a bias of V=80 mV to the sample. Similar force maps are obtained at zero bias [21]. The plot in (b) shows the value of the conductance at zero force. G is plotted in logarithmic scale in units of the quantum of conductance $G_0 = 2e^2/h = (12906\ \Omega)^{-1}$. Both force and conductance are obtained after deconvolution of the tip oscillation [19, 31]. (c) Conductance, force and energy curves taken at the C=C bond with a CO tip. A change in conductance occurs at the energy minimum.

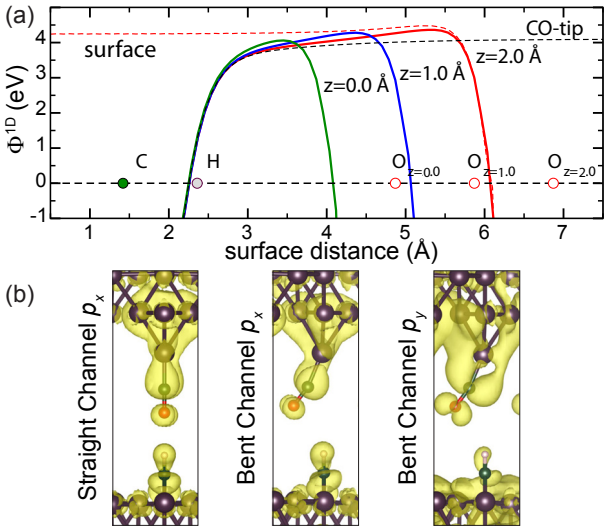

FIG. 4: (a) Development of the electrostatic (Hartree) potential felt by electrons in the gap between the tip and the acetylene molecule on the surface as the tip gradually approaches to the surface. The potentials are plotted along the CO molecular axis. Dashed black and red lines plot the electrostatic potential of the free standing surface and CO-tip respectively. The position of individual atoms of the acetylene molecule on the surface and oxygen atom on tip at different tip-sample distances is schematically presented. All potentials are rendered with respect to the Fermi level. (b) Spatial distribution of the dominant eigen-channels at the Fermi energy for straight and bent CO-configuration at the same tip-sample distance z=0 Å.

molecules approach, leading to increasing polarization of opposite sign of both CO and C_2H_2, and explaining the build up of attractive, short-range electrostatic forces.

The charge rearrangement in the absence of wavefunction overlap is due to the existence of a finite dipole moment of the molecules, and their effect on the local work-functions of tip and sample: the CO molecule increases the copper work-function, whereas C_2H_2 decreases it [21]. The result is the existence of a finite electric field E_{loc} at the tunneling junction, which increases and enhances the electrical polarization of the molecules as they are approached. In fact, by applying an homogeneous electric field of E_z=0.1 eV/Å to either CO-tip or C_2H_2 sample we obtain a similar charge redistribution as when the tip is at z_0 (see dashed lines in $\Delta\rho$ plots of Fig. 2c). The electrostatic field E_{loc} built up at the junction causes variations of the local contact potential difference with the tip-sample separation, which are crucial for interpreting local Kelvin Probe Force Spectroscopy measurements [4, 28, 29].

Correlation of forces with charge transport: The absence of covalent character at the CO-C_2H_2 bond implies that a tunneling mechanism may be required to describe the charge transport across the junction. Therefore, the electrical conductance is expected to be low but very sensitive to small forces affecting the molecular junction. To obtain the conductance of a relaxed CO-C_2H_2 molecular junction, we measured simultaneously the linear conductance (G) and Δf as a CO-tip was approached at different sites along an acetylene molecule. The resulting G(x,z) and F_z(x,z) maps are shown in Fig. 3. The G(x,z) map corroborates that the conductance over the C=C bond of acetylene is the largest along the molecule [27, 32]. The profile of bond equilibrium distance $z_0(x)$ (white contour in Fig. 3b) shows a minimum at the C=C bond, reflecting that at the center forces have a shorter range (and are more attractive than over the H atoms [21]) probably due to the H atoms bending upwards. In the inset of Fig. 3b we plot the conductance values at the $z_0(x)$ positions. The conductance of a CO molecule bonding to the C=C site of acetylene turns out to be a factor of two larger than when contacting the hydrogen atoms.

The measured tunneling conductance at the $F_z(z_0)$=0 turning point amounts to $\sim 10^{-3} G_0$ ($G_0 = e^2/\pi\hbar$) (Fig. 3b and 3c). This low value confirms the persistence of a tunneling barrier at this contact point. In Fig. 4a, we show the Hartree potential (the electrostatic potential felt by electrons) calculated in the gap between the CO at the tip and the C_2H_2 molecule. The tunneling barrier does not collapse during the approach, and remains substantially above the Fermi level even when the

force turning point z_0 is reached and forces become repulsive. The calculated conductance is in all the process far below one quantum of conductance. This behavior is thus a characteristic of the non-covalent character of the bond, and contrasts with the case of metallic atomic contacts, where the tunneling barrier was found to collapse in contact [3] and the transport becomes ballistic.

Bending of the CO molecule: Compressing the molecular junction into the repulsive regime leads to a change of slope in the G(z) plot (Fig. 3c) which resembles the transition to ballistic transport of metallic and molecular point contacts [33, 34]. However, we note that this flattening coincides with an inflection also visible in the short-range F-z force curve, and responsible of the characteristic peak observed in the Δf plots of Fig. 2a and in [21]. Thus, the flattening of the G(z) plot is a consequence of a mechanical rearrangement of the junction to relax repulsive forces [7]. The most probable change is the bending of the tip apex. It has been shown that a CO molecule on the apex can be easily tilted away from its original direction in response to lateral attractive forces [35, 36]. In our case, sufficiently large repulsive forces in the junction (up to 50 pN, as seen in Fig. 2 and [21]) induce the lateral bending of the CO molecule [37] when approaching potential saddle points such as the C=C bond. In this way, the CO molecule amplifies the response of the AFM to a potential landscape. This mechanism has been identified as responsible for intra-, and intermolecular bond contrast in constant height AFM images [38–41]

The bending of the CO molecule affects the electron tunneling in two ways: First, it avoids the collapse of the tunneling barrier as the tip approaches. Second, it reduces the symmetry of the junction. To evaluate the impact of a reduced symmetry on tunneling, we calculated the transmission function of the different channels using non-equilibrium Green's function formalism implemented in the Smeagol code [42] together with the Fireball code [43]. Interestingly, the bending of the CO molecule over the C=C nodal plane leads to a swap of the leading transmission channels. For a straight CO tip we find that the eigenchannel with p_x-character is responsible for the majority of conductance (x direction along the C_2H_2 axis), in agreement with [27]. The bending of the CO tip reduces drastically the transmission through this channel, while another channel with prevailing p_y orbital character dominates the tunneling. For a straight CO molecule this channel was not active in the charge transport because its nodal plane lies along the C_2H_2 axis. When the symmetry is reduced, one of its lobes couples with the C_2H_2 orbitals (Fig. 4c), allowing the flow of charge (see section S3 in SM [21]). The consequence of the tip bending is thus a change of symmetry of the main tunneling channel, which should lead to a change in conductance contrast for short distances.

In summary, the short range interactions between a small hydrocarbon such as acetylene and a CO molecule at the tip of an AFM show a weak attractive component originating from their intrinsic dipole moment and from the charge redistribution upon chemisorption. The electrical polarization of the molecules rises as they are brought into contact, leading to a gradual increase in the contact potential difference. However, the two molecules are chemically passive, and no chemical bond was formed even when they enter in a regime of repulsive forces. The lack of chemical activity protects the tunneling barrier from collapsing and allows to perform stable force and conductance mapping in the regime of repulsive forces. We found that repulsive forces cause the bending of the CO molecule and the decrease of the stiffness of the junction.

We thank Peter Saalfrank for discussions. The research was supported by DFG (grants SPP1243 and Sfb 658), the Czech Science Foundation (GAČR), project 14-02079S, and the Spanish MINECO (grant No. MAT2013-46593-C6-01). MC acknowledges research fellowship from the Alexander von Humboldt Foundation.

[1] N. Agrait, A. Levy-Yeyati, J.M. van Ruitenbeek, Phys. Reps. **377**, 81 (2003).
[2] U. Dürig, O. Züger, D.W. Pohl, Phys. Rev. Lett. **65**, 349 (1990).
[3] M. Ternes, C. González, C. P. Lutz, P. Hapala, F. J. Giessibl, P. Jelínek, A. J. Heinrich, Phys. Rev. Lett. **106**, 016802 (2011).
[4] S. Sadewasser, P. Jelinek, C.-K. Fang, O. Custance, Y. Yamada, Y. Sugimoto, M. Abe, S. Morita, Phys. Rev. Lett. **103**. 266103 (2009).
[5] P. Jelínek, M. Svec, P. Pou, R. Perez, V.Cháb, Phys. Rev. Lett **101**, 176101 (2008).
[6] A. Shiotari, Y. Kitaguchi, H. Okuyama, S. Hatta, T. Aruga, Phys. Rev. Lett **106**, 156104 (2011).
[7] A. Yazdani, D. M. Eigler, and N. D. Lang, Science **272**, 1921 (1996).
[8] V. Coropceanu, J. Cornil, D.A. da Silva Filho, Y. Olivier, R. Silbey, J.L. Brédas, Chemical reviews, 107, 926 (2007).
[9] L. Gross, F. Mohn, N. Moll, P. Liljeroth, G. Meyer, Science **325**, 1110 (2009).
[10] L. Gross, F. Mohn, N. Moll, G. Meyer,R. Ebel, W. Abdel-Mageed, M. Jaspars, Nat. Chem. **2**, 821 (2010).
[11] F. Mohn, L. Gross, G. Meyer, App. Phys. Lett. **99**, 053106 (2011).
[12] G. Kichin, C. Weiss, C. Wagner, S. Tauz, R. Temirov, J. Am. Chem. Soc. **133**, 16847 (2011).
[13] N. Pavliček, B. Fleury, M. Neu, J. Niedenführ, C. Herranz-Lancho, M. Ruben, J. Repp, Phys. Rev. Lett. **108**, 086101 (2012).
[14] D. G. de Oteyza, P. Gorman, Y.-C. Chen, S. Wickenburg, A. Riss, D. J. Mowbray, G. Etkin, Z. Pedramrazi, H.-Z. Tsai, A. Rubio, M. F. Crommie, F. R. Fischer, Science **340**, 1434 (2013).
[15] A. Riss, S. Wickenburg, P. Gorman, L. Z. Tan, H.-Z. Tsai, D. G. de Oteyza, Y.-C. Chen, A. J. Bradley, M. M. Ugeda, G. Etkin, S. G. Louie, F. R. Fischer, M. F. Crommie, Nano Lett. **14**, 2251 (2014).

[16] F. J. Giessibl, App. Phys. Lett. **76**, 1470 (2000).

[17] T. R. Albrecht, P. Grütter, D. Horne, D. Rugar, J. App. Phys. **69**, 668 (1991).

[18] The qPlus sensor in this experiment is characterized by: a spring constant $k_0 \approx$ 1.8 kN/m), resonance frequency of f_0=20.7 kHz and quality factor Q$\approx 1.6\times10^4$. The data here presented are measured with a constant oscillation amplitude of $A_{osc} \approx$ 30pm. The tip-sample distance is given as the real piezo vertical displacement with respect to the STM set point taken on the Cu substrate.

[19] J. E. Sader, S. P. Jarvis, App. Phys. Lett. **84**, 1801 (2004).

[20] Z. Sun, M. P. Boneschanscher, I. Swart, D. Vanmaekelbergh, P. Liljeroth, Phys. Rev. Lett. **106**, 046104 (2011).

[21] See Supplementary Online Material.

[22] W. Liu, J. S. Lian, Q. Jiang, J. Phys. Chem. C **111**, 18189 (2007).

[23] L. Bartels, G. Meyer, K. -H. Rieder, App. Phys. Lett. **71**, 213 (1997).

[24] S. Ishi, Y. Ohno, B. Viswanathan, Surf. Sci. **162**, 349 (1985).

[25] B. C. Stipe, M. A. Rezaei, W. Ho, Phys. Rev. Lett. **81**, 1263 (1998).

[26] Y. Konishi, Y. Sainoo, K. Kanazawa, S. Yoshida, A. Taninaka, O. Takeuchi, H.Shigekawa, Phys. Rev. B **71**, 193410 (2005).

[27] L. Gross, N. Moll, F. Mohn, A. Curioni, G. Meyer, F. Hanke, M. Persson, Phys. Rev. Lett. **107**, 086101 (2011).

[28] F. Mohn, L. Gross, N. Moll, G. Meyer Nature Nanotechnology **74**, 227 (2012).

[29] B. Schuler, S.-X. Liu, Y. Geng, S. Decurtins, G. Meyer, L. Gross, Nano Letters, DOI: 10.1021/nl500805x (2014).

[30] M. Schneiderbauer, M. Emmrich, A. J. Weymouth, F. J. Giessibl, Phys. Rev. Lett. **112**, 166102 (2014).

[31] J. E. Sader, Y. Sugimoto, App. Phys. Lett. **97**, 043502 (2010).

[32] N. Pavliček, I. Swart, J. Niedenführ, G. Meyer, J. Repp, Phys. Rev. Lett. **110**, 136101 (2013).

[33] N. Néel, J. Kröger, L. Limot, T. Frederiksen, M. Brandbyge, R. Berndt, Phys. Rev. Lett. **98**, 065502 (2007).

[34] G. Schulze, K. J. Franke, A. Gagliardi, G. Romano, C.S. Lin, A.L. Rosa, T.A. Niehaus, Th. Frauenheim, A. Di Carlo, A. Pecchia, J. I. Pascual, Phys. Rev. Lett. **100**, 136801 (2008).

[35] M. Neu, N. Moll, L. Gross, G. Meyer, F. J. Giessibl, J. Repp, Phys. Rev. B **89**, 205407 (2014).

[36] A. J. Weymouth, T. Hofmann, F. J. Giessibl, Science **343**, 1120 (2014).

[37] From our DFT simulations, we obtain that the CO molecule undergoes the larger structural relaxation (165 pm lateral relaxation), whereas the relaxation of all acetylene atoms is less than 3 pm.

[38] L. Gross, F. Mohn, N. Moll, B. Schuler, A. Criado, E. Guitián, D. Pea, André Gourdon, G. Meyer, Science **337**, 1326 (2012).

[39] A.M. Sweetman1, et al. Nature Comm. 5, 3931 (2014).

[40] P. Hapala, et al. Phys. Rv. B 90, 085421 (2014).

[41] S.K. Hämäläinen et al. Phys. Rev. Lett. 113, 186102 (2014).

[42] A. R. Rocha, V. M. García-Suárez, S. Bailey, C. Lambert, J. Ferrer, S. Sanvito, Phys. Rev. B **73**, 085414 (2006).

[43] J. P. Lewis et al, Phys. Stat. Sol. b **248**, 1989 (2011).